Title: A Data-driven Approach to Petroleum Engineering Problems

Author: Rong Lu

Affiliation: Colorado School of Mines

Email: rlu@mines.edu

Statement: this paper is a non-peer reviewed preprint submitted to EarthArXiv.

Please add comments to the page: "This is a late posting of an old paper (year 2017, Colorado School of Mines)"

A Data-driven Approach to Petroleum Engineering Problems

Rong Lu

2017

1 Summary

In this work, a data-driven approach is taken to tackle problems in Petroleum Engineering domain, for both conventional and unconventional reservoirs.

Conventional reservoirs face the problem of losing energy for flowing after a few years of production, thus operators choose to inject water and inject CO_2 as a secondary and tertiary recovery method. The question of interest is that how injection scheme correlates with production responses. As shown from this work, supervised learning (support vector machines) can answer the question and come up with predictive models.

On the other hand, unconventional oil and gas resources development has gained much more attention since the last decade, due to the advancement in hydraulic fracturing (HF, or "frac") technology. In order to develop shale gas reservoirs, which have extremely low permeability, HF has to be applied. In the process fluids and solids under high pressure are pumped into the formation to break the rock. As fractures are created, more reservoir contact are obtained and the shale gas would flow through the fractures to the wellbore. Two questions the industry are interested in are, where to frac the wells in unconventional shale plays, and with so many completion and stimulation parameters whether there exists any hidden patterns. The two aspects are approached by both supervised (linear regression) and unsupervised learning (cluster analysis) in the following.

2 Dataset Description

The conventional oil reservoir dataset is a time series covering from year 1967 to 2015, consisting of 585 timestamps. For the most part, data at each timestamp represents a monthly reporting, on gas/oil/water production rates and water/CO_2 injection rates. The records are for individual wells and there are 521 wells in total. The wells are producing from Bell Creek Field, Montana. The data was provided by Denbury Resources Inc., and it can be shared. A screenshot of part of the dataset is shown in Figure 6 (Appendix A).

The unconventional reservoir dataset is a well completion database. It contains more than 300 shale gas wells drilled in Cana Woodford Shale in Oklahoma; for each well, there are completion and HF job parameters, and initial production data up to the first 90 days. A screenshot of part

of the database is shown in Figure 7 (Appendix B). The dataset was provided by Devon Energy Corporation through a research project in Fracturing, Acidizing, Stimulation Technology (FAST) Consortium at Colorado School of Mines. All the data can be used for machine learning purposes except that well identifier information (name and location) cannot be disclosed.

Both datasets are in the form of Microsoft Excel.

3 Problem Formulation and Methodology

3.1 Oil Production's Response to Water Injection

Bell Creek Field started production activity in 1967, a few years after which water injection was initiated in order to maintain reservoir pressure and serves as a secondary recovery method ("pushing oil out"). How water injection impacts oil production is of interest, because the knowledge gained will also guide the CO_2 injection scheme (tertiary recovery method) which just started in May 2013.

In this work all the 521 wells are treated as one system, which means necessary data pre-processing needs to done to accumulate the rates for the available wells at each timestamp. Interested readers can refer to Figure 8 (Appendix C) as a visualization of the history. It is natural to proceed under supervised learning framework since the variable of interest is clear, being oil production. The way the raw data (in time-series) is converted into a supervised learning problem is shown in Figure 1. In this work two different time lags are chosen, and the states at each previous timestamp are used as features, shown in Table 1.

Table 1: Input and Output Space for Supervised Learning

Features	Output
Oil Production $(t-1)$	Oil Production $(t+1)$
Water Injection $(t-1)$	
Oil Production (t)	
Water Injection (t)	

The regression learners are chosen to be support vector machines (SVMs) (Pedregosa et al., 2011). Three different kernels are used for comparison: radial basis function (RBF), linear, and third-degree polynomial.

Time	Observations
0	x0
1	x1
2	x2
3	x3
4	x4
5	x5

Time	Observations
0	x0
1	x1
2	x2
3	x3
4	x4
5	x5

Figure 1: This demonstrates how a time series can be converted into a supervised learning problem. By making a copy of the original data and "pulling" one of them in time scale (here shows pulling one time step as a lag distance), the input (in solid box; indicating previous observations) and the output (in dashed box; indicating future observations) are created.

3.2 Selecting New Well Locations

In this section how to find new locations for HF wells is discussed. From the literature (Krivoruchko and Wood, 2014), a well performance index (WPI) is used to estimate how much production potential a well has, using the initial 90 days' production and pressure data:

$$\text{WPI} = \sum_{i=1}^{90} \text{dailyProdRate}_i \times \text{dailyPressure}_i$$

It is assumed in this work that pressure is constant over the first 90 days and that fracture pressure can be used for estimation purposes, then the equation becomes (the hat indicates it is an estimator for the true WPI):

$$\widehat{\text{WPI}} = \text{avgProdRateFirst90Days(MCFE/day)} \times 90 \times \text{fracGradient} \times \text{TVD}$$

Now all the information needed is available from the dataset. Interested readers can refer to Figure 9 (Appendix D) as a visualization of the spatial distributions and relative values of $\widehat{\text{WPI}}$. The approach for prediction, known as "kriging" in mining industry, is essentially a linear estimator using the known information. The core idea is to assign weights w_i to each known data point $z(x_i)$ located at

x_i, and by applying a linear summation the property value at unsampled location x_0 is obtained:

$$\widehat{Z}(x_0) = \begin{bmatrix} w_1 & w_2 & \dots & w_n \end{bmatrix} \cdot \begin{bmatrix} z_1 \\ z_2 \\ \vdots \\ z_n \end{bmatrix} = \sum_{i=1}^{n} w_i(x_0) \times Z(x_i)$$

Weights, w_i, are determined by minimizing variance of estimation (Pebesma, 2004). The performance of this linear estimator is measured by RMSE after doing leave-one-out cross validation.

3.3 Grouping of Hydraulic Fracturing Wells

Continuing with Cana Field dataset, the operator would like to know if there exists hidden grouping among the hydraulically fractured wells. Along with this goal, unsupervised learning is also a great tool for exploratory data analysis (EDA), as its output might be able to direct the future supervised learning. Here 4 attributes are picked, shown in Table 2 (only demonstrating a part of the data).

Table 2: Clustering Dataset Demonstration

Well Name	Frac Cost	Production Rate	# of stgs	total sand
A	$3,343,191	6,555	18	4,507,380
B	$3,700,368	7,603	16	4,146,260
C	$2,951,079	6,993	16	3,424,965
D	$3,136,772	5,991	16	3,266,746

The workflow is shown in Figure 2.

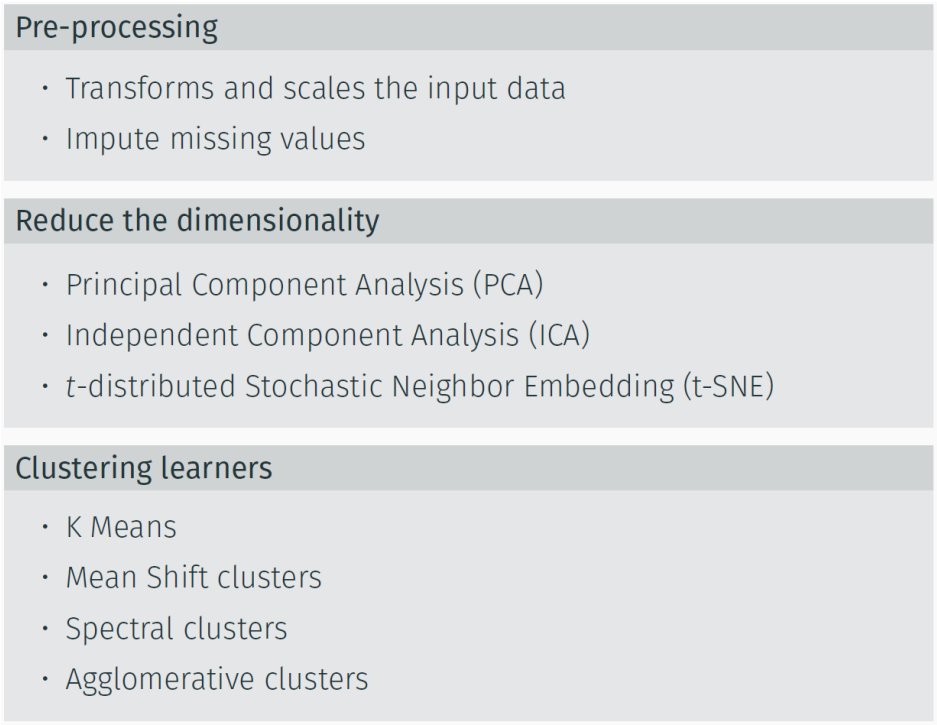

Figure 2: The workflow starts from top, continuing to bottom. Different dimensionality reduction methods and clustering algorithms are tried.

4 Results and Verifications

4.1 Oil Production's Response to Water Injection

The results of modeling oil production as a response of water injection are shown in Figure 3.

4.2 Selecting New Well Locations

The estimation of WPI values at unsampled locations along with recommendations of new well locations are shown in Figure 4.

4.3 Grouping of Hydraulic Fracturing Wells

Currently the number of clusters is chosen to be two. Following the workflow outlined above, data are plotted for the two principal components, with different colors indicating different classes predicted (Figure 5).

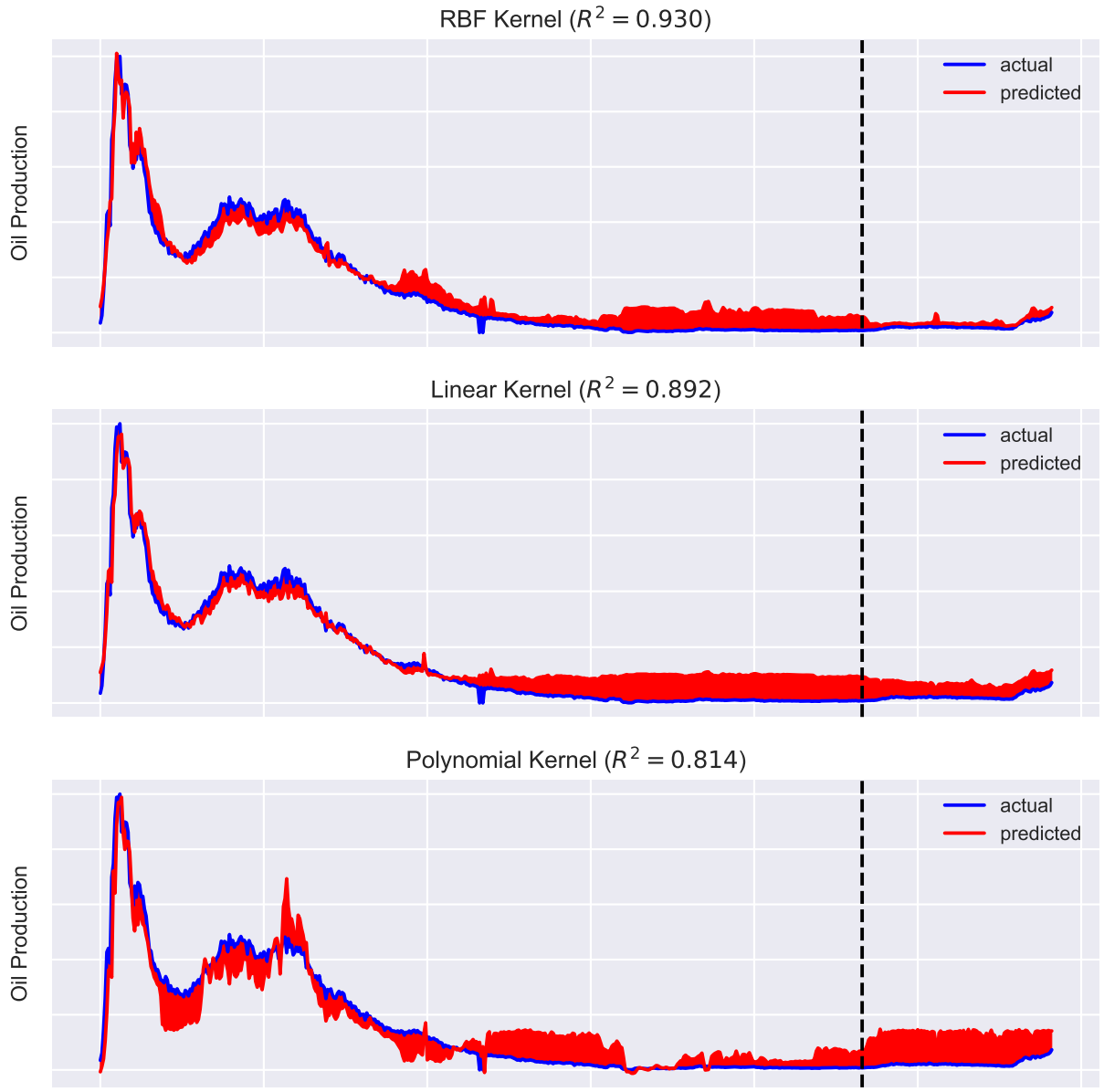

Figure 3: Three SVMs using different kernels are trained for the given dataset. The horizontal axis shows the time span from year 1967 to 2015. It can be seen that RBF kernel has the best performance in terms of R^2 score (the score is from testing on the whole dataset). The shaded area indicate where the prediction does not match the true value. The dashed lines indicate the training/testing sets split (80/20 split). Please note when handling time series, previous observations have to be used as training, while testing against latter observations. Thus traditional cross-validation with shuffling is not applied here.

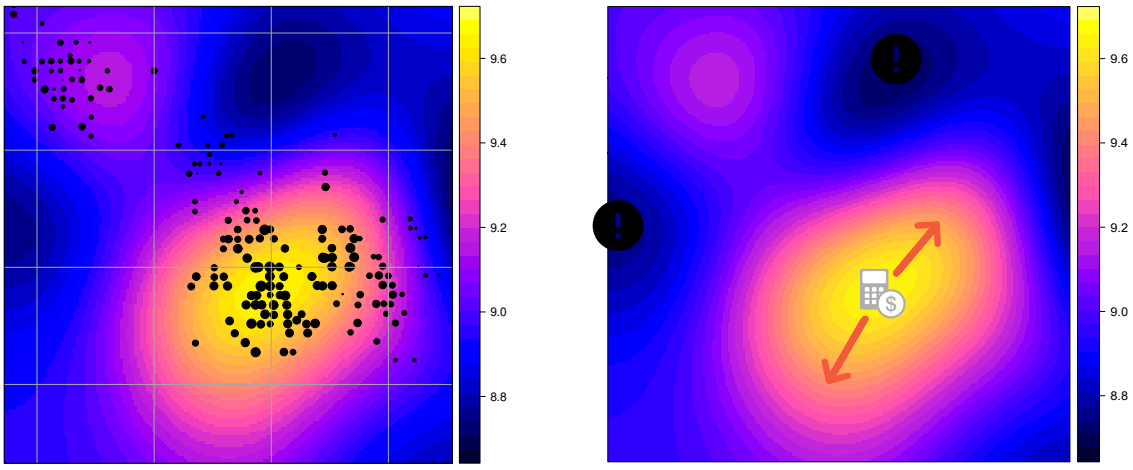

(a) The prediction matches well with the original data, as the majority of larger points fall on the lighter color zone, which indicates higher WPI values.

(b) New wells are recommended to be located at the "dollar sign" area, whereas the zones showing warnings have lower producing potentials.

Figure 4: Linear estimations of WPI across the region. RMSE = 0.249.

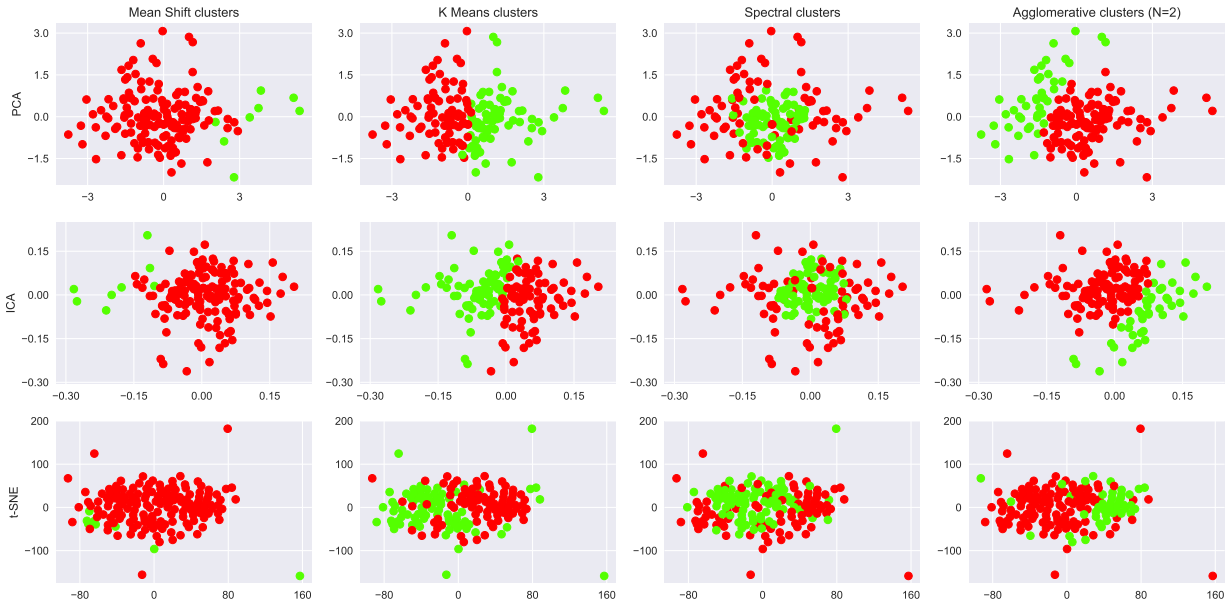

Figure 5: Clear cluster separations are not found under current dimensionality reduction and clustering scheme.

5 Conclusions and Recommendations

5.1 Conclusions

It is shown that data-driven approaches can have very good performance on petroleum engineering domain datasets. Both predictive models of oil production for Bell Creek Field and new well locations for Cana Field have been proposed, using supervised learning techniques.

5.2 Recommendations

As part of the future work, LSTM network, a type of recurrent neural network, will be leveraged for time series predictions. From the research it seems to perform very well on time-series. Regarding the ongoing cluster analysis, different number of principal components will be tried and then clustering results visualized.

Acknowledgments

I would like to thank Dr. Wendy Fisher for her advice. I would also like to thank Denbury and Devon for providing me with the data.

References

Krivoruchko, Konstantin and Nathan Wood (2014). "Using Multivariate Interpolation for Estimating Well Performance Understanding Multivariate Interpolation". In: *ArcUser*.

Pebesma, Edzer J. (2004). "Multivariable geostatistics in S: the gstat package". In: *Computers & Geosciences* 30, pp. 683–691.

Pedregosa, F. et al. (2011). "Scikit-learn: Machine Learning in Python". In: *Journal of Machine Learning Research* 12, pp. 2825–2830.

Appendices

A Screenshot of Part of the Conventional Reservoir Database

	A	B	C	D	E	F	G	H	I	J	K	L
1	FIELD	SUMMARY	SEQNUM	DRI_LEASE	RESERVOIR	API	P_DATE	OIL	GAS	WATER	WATERINJ	CO2TOTINJ
58919	BELL CREEK	N	60090	BCU D 05-05	MUD	25075213650000	31-Jul-73	1,651	83	51		
58920	BELL CREEK	N	60090	BCU D 05-05	MUD	25075213650000	31-Aug-73	2,925	146	91		
58921	BELL CREEK	N	60090	BCU D 05-05	MUD	25075213650000	30-Sep-73	2,210	111	91		
58922	BELL CREEK	N	60090	BCU D 05-05	MUD	25075213650000	31-Oct-73	3,733	187	198		
58923	BELL CREEK	N	60090	BCU D 05-05	MUD	25075213650000	30-Nov-73	4,396	110	44		
58924	BELL CREEK	N	55710	BCU D 05-05	MUD	25075213650000	31-Mar-13	0	0	0	5,163	0
58925	BELL CREEK	N	55710	BCU D 05-05	MUD	25075213650000	30-Apr-13	0	0	0	4,534	0
58926	BELL CREEK	N	55710	BCU D 05-05	MUD	25075213650000	31-May-13	0	0	0	6,617	7,565
58927	BELL CREEK	N	55710	BCU D 05-05	MUD	25075213650000	30-Jun-13	0	0	0	0	31,639
58928	BELL CREEK	N	55710	BCU D 05-05	MUD	25075213650000	31-Jul-13	0	0	0	0	28,511
58929	BELL CREEK	N	55710	BCU D 05-05	MUD	25075213650000	31-Aug-13	0	0	0	0	51,533
58930	BELL CREEK	N	55710	BCU D 05-05	MUD	25075213650000	30-Sep-13	0	0	0	0	68,823
58931	BELL CREEK	N	55710	BCU D 05-05	MUD	25075213650000	31-Oct-13	0	0	0	0	83,687
58932	BELL CREEK	N	55710	BCU D 05-05	MUD	25075213650000	30-Nov-13	0	0	0	0	25,939
58933	BELL CREEK	N	55710	BCU D 05-05	MUD	25075213650000	31-Dec-13	0	0	0	0	34,789
58934	BELL CREEK	N	55710	BCU D 05-05	MUD	25075213650000	31-Jan-14	0	0	0	0	58,197
58935	BELL CREEK	N	55710	BCU D 05-05	MUD	25075213650000	28-Feb-14	0	0	0	0	91,640
58936	BELL CREEK	N	55710	BCU D 05-05	MUD	25075213650000	31-Mar-14	0	0	0	0	84,945
58937	BELL CREEK	N	55710	BCU D 05-05	MUD	25075213650000	30-Apr-14	0	0	0	0	87,807
58938	BELL CREEK	N	55710	BCU D 05-05	MUD	25075213650000	31-May-14	0	0	0	0	105,587
58939	BELL CREEK	N	55710	BCU D 05-05	MUD	25075213650000	30-Jun-14	0	0	0	0	120,065
58940	BELL CREEK	N	55710	BCU D 05-05	MUD	25075213650000	31-Jul-14	0	0	0	0	123,236
58941	BELL CREEK	N	55710	BCU D 05-05	MUD	25075213650000	31-Aug-14	0	0	0	0	140,976
58942	BELL CREEK	N	55710	BCU D 05-05	MUD	25075213650000	30-Sep-14	0	0	0	0	121,757
58943	BELL CREEK	N	55710	BCU D 05-05	MUD	25075213650000	31-Oct-14	0	0	0	0	110,092
58944	BELL CREEK	N	55710	BCU D 05-05	MUD	25075213650000	30-Nov-14	0	0	0	0	110,395
58945	BELL CREEK	N	55710	BCU D 05-05	MUD	25075213650000	31-Dec-14	0	0	0	0	112,824
58946	BELL CREEK	N	55710	BCU D 05-05	MUD	25075213650000	31-Jan-15	0	0	0	0	81,488
58947	BELL CREEK	N	55710	BCU D 05-05	MUD	25075213650000	28-Feb-15	0	0	0	0	99,115
58948	BELL CREEK	N	55710	BCU D 05-05	MUD	25075213650000	31-Mar-15	0	0	0	0	121,381
58949	BELL CREEK	N	55710	BCU D 05-05	MUD	25075213650000	30-Apr-15	0	0	0	10,459	50,732
58950	BELL CREEK	N	55710	BCU D 05-05	MUD	25075213650000	31-May-15	0	0	0	13,562	13,949
58951	BELL CREEK	N	55710	BCU D 05-05	MUD	25075213650000	30-Jun-15	0	0	0	0	113,158
58952	BELL CREEK	N	55710	BCU D 05-05	MUD	25075213650000	31-Jul-15	0	0	0	0	141,986
58953	BELL CREEK	N	55710	BCU D 05-05	MUD	25075213650000	31-Aug-15	0	0	0	12,196	53,505
58954	BELL CREEK	N	55710	BCU D 05-05	MUD	25075213650000	30-Sep-15	0	0	0	6,047	94,294
58955	BELL CREEK	N	55710	BCU D 05-05	MUD	25075213650000	31-Oct-15	0	0	0	5,969	85,347
58956	BELL CREEK	N	55710	BCU D 05-05	MUD	25075213650000	30-Nov-15	0	0	0	5,260	101,131
58957	BELL CREEK	N	55710	BCU D 05-05	MUD	25075213650000	31-Dec-15	0	0	0	10,953	59,470
58958	BELL CREEK	N	27402	BCU D 56-08	MUD	25075213660000	31-Mar-68	4,663	0	0	0	
58959	BELL CREEK	N	27402	BCU D 56-08	MUD	25075213660000	30-Apr-68	9,322	0	0	0	
58960	BELL CREEK	N	27402	BCU D 56-08	MUD	25075213660000	31-May-68	7,892	0	34	0	

Figure 6: This shows part of the conventional oil reservoir dataset.

B Screenshot of Part of the Unconventional Reservoir Database

B	CN	CO	CP	CQ	CR	CS	CT	CU	CV	CW	CX	CY	CZ
Well Stage	Pad Volume	Mesh sz 1	Fluid for Prop 1	Prop 1 Type	Max Prop Conc. 1	Planned 1 Prop Quant	Actual 1 Prop Quant	Mesh sz 2	Fluid for Prop 2	Prop 2 Type	Max Prop Conc. 2	Planned 2 Prop Quant	Actual 2 Prop Quant
5	0	LD 60	0	Carbo Ceramics		300,500	301,180	40/70	0	Hexion Primie Plus		686,500	689,880
1	0	LD 60	0	Carbo Ceramics		60,100	60,640	40/70	0	Hexion Primie Plus		137,300	140,318
2	0	LD 60	0	Carbo Ceramics		60,100	60,428	40/70	0	Hexion Primie Plus		137,300	142,062
3	0	LD 60	0	Carbo Ceramics		60,100	63,206	40/70	0	Hexion Primie Plus		137,300	141,748
4	0	LD 60	0	Carbo Ceramics		60,100	60,800	40/70	0	Hexion Primie Plus		137,300	136,600
5	0	LD 60	0	Carbo Ceramics		60,100	56,106	40/70	0	Hexion Primie Plus		137,300	129,152
5	0	LD 50	0	Carbo Ceramics		300,500	302,480	40/70	0	Hexion Primie Plus		686,500	677,304
1	0	LD 50	0	Carbo Ceramics		60,100	63,976	40/70	0	Hexion Primie Plus		137,300	130,400
2	0	LD 50	0	Carbo Ceramics		60,100	60,308	40/70	0	Hexion Primie Plus		137,300	137,600
3	0	LD 50	0	Carbo Ceramics		60,100	60,373	40/70	0	Hexion Primie Plus		137,300	134,162
4	0	LD 50	0	Carbo Ceramics		60,100	61,173	40/70	0	Hexion Primie Plus		137,300	139,649
5	0	LD 50	0	Carbo Ceramics		60,100	56,650	40/70	0	Hexion Primie Plus		137,300	135,493
6	0	35/140	0	Saint-Gobain Interprop		360,600	264,200	40/70	0	Hexion Primie Plus		830,700	579,393
1	0	35/140	0	Saint-Gobain Interprop		60,100	15,378	40/70	0	Hexion Primie Plus		138,450	0
2	0	35/140	0	Saint-Gobain Interprop		60,100	63,281	40/70	0	Hexion Primie Plus		138,450	141,120
3	0	35/140	0	Saint-Gobain Interprop		60,100	59,000	40/70	0	Hexion Primie Plus		138,450	139,550
4	0	35/140	0	Saint-Gobain Interprop		60,100	57,341	40/70	0	Hexion Primie Plus		138,450	157,223
5	0	35/140	0	Saint-Gobain Interprop		60,100	3,097	40/70	0	Hexion Primie Plus		138,450	0
6	0	35/140	0	Saint-Gobain Interprop		60,100	66,103	40/70	0	Hexion Primie Plus		138,450	141,500
8	0	100	0	White		0	102,521	35/140	0	Saint-Gobain Interprop		478,672	414,309
1	0	100	0	White		0	2,241	35/140	0	Saint-Gobain Interprop		59,834	0
2	0	100	0	White		0	15,845	35/140	0	Saint-Gobain Interprop		59,834	47,814
3	0	100	0	White		0	16,035	35/140	0	Saint-Gobain Interprop		59,834	59,737
4	0	100	0	White		0	18,680	35/140	0	Saint-Gobain Interprop		59,834	70,208
5	0	100	0	White		0	19,000	60/120	0	Saint-Gobain Interprop		59,834	46,316
6	0	100	0	White		0	15,000	60/120	0	Saint-Gobain Interprop		59,834	59,769
7	0	100	0	White		0	15,720	60/120	0	Saint-Gobain Interprop		59,834	53,200
8	0	100	0	White		0	0	60/120	0	Saint-Gobain Interprop		59,834	77,265
8	0	100	0	White		251,488	171,350	35/140	0	Saint-Gobain Interprop		215,944	169,778
1	0	100	0	White		31,436	1,990	35/140	0	Saint-Gobain Interprop		26,993	0
2	0	100	0	White		31,436	2,500	35/140	0	Saint-Gobain Interprop		26,993	0
3	0	100	0	White		31,436	32,100	35/140	0	Saint-Gobain Interprop		26,993	25,745
4	0	100	0	White		31,436	11,500	35/140	0	Saint-Gobain Interprop		26,993	26,219
5	0	100	0	White		31,436	31,502	35/140	0	Saint-Gobain Interprop		26,993	27,771
6	0	100	0	White		31,436	30,000	35/140	0	Saint-Gobain Interprop		26,993	30,450
7	0	100	0	White		31,436	30,411	35/140	0	Saint-Gobain Interprop		26,993	28,749

Figure 7: This shows part of the unconventional oil reservoir dataset.

C Production and Injection History of Bell Creek Field

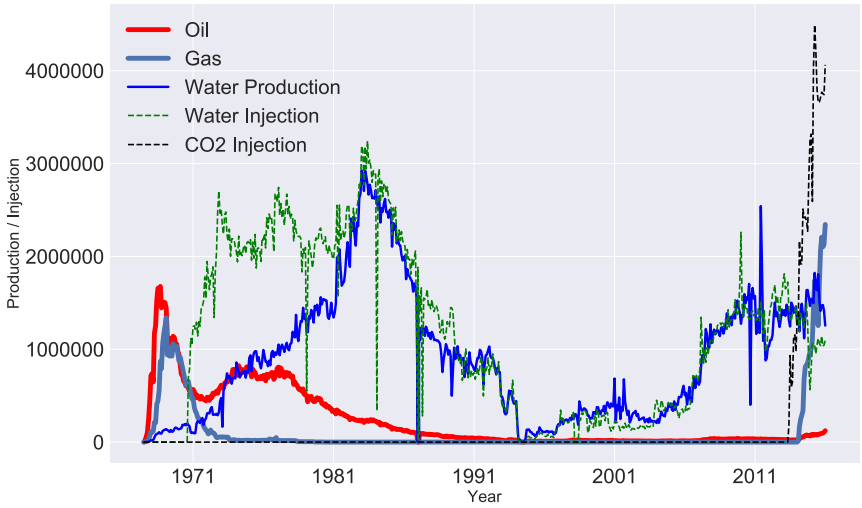

Figure 8: This shows Bell Creek Field's production and injection activities in time series.

D WPI Samples of Cana Field

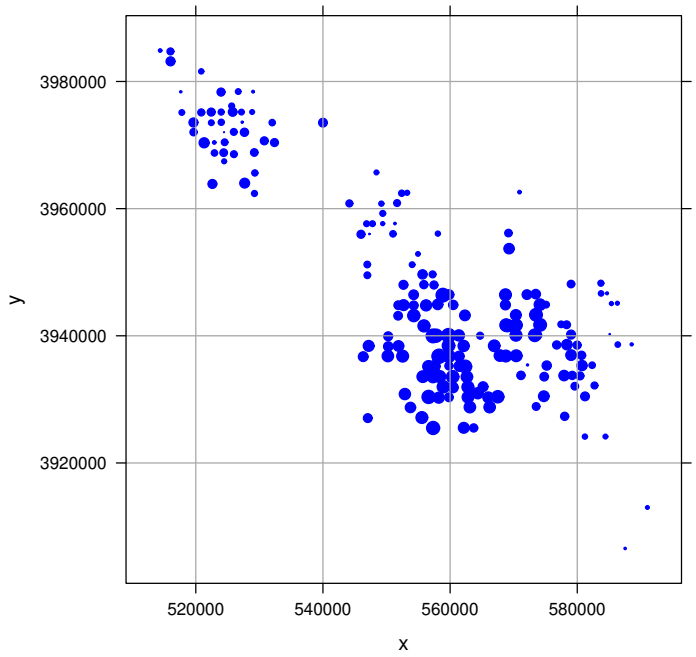

Figure 9: This shows a bubble plot for WPI samples. Larger points indicate larger WPI values. X and Y axes are for easting and northing (units in meters), respectively.